Neuron, Volume *108*

Supplemental Information

Differential Relation between Neuronal and Behavioral Discrimination during Hippocampal Memory Encoding

Manuela Allegra, Lorenzo Posani, Ruy Gómez-Ocádiz, and Christoph Schmidt-Hieber

Figure S1

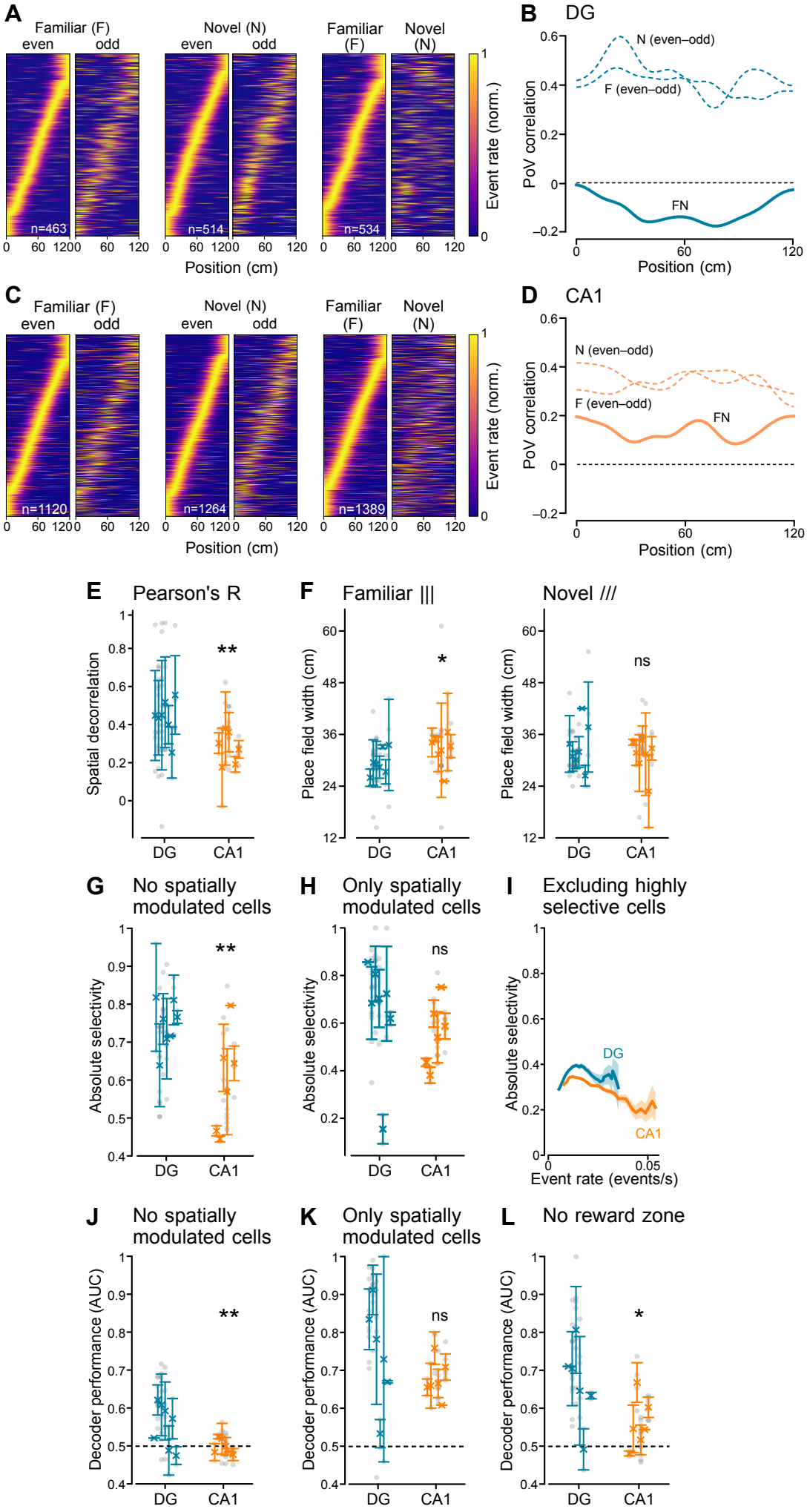
A
Familiar (F)
even
odd
Novel (N)
even
odd
Familiar (F)
Novel (N)
n=463
n=514
n=534
Event rate (norm.)
Position (cm)
B
DG
N (even–odd)
F (even–odd)
FN
PoV correlation
Position (cm)
C
n=1120
n=1264
n=1389
D
CA1
E
Pearson's R
Spatial decorrelation
**
DG
CA1
F
Familiar |||
Place field width (cm)
*
Novel ///
ns
G
No spatially modulated cells
Absolute selectivity
**
H
Only spatially modulated cells
ns
I
Excluding highly selective cells
Event rate (events/s)
J
No spatially modulated cells
Decoder performance (AUC)
**
K
Only spatially modulated cells
ns
L
No reward zone
*

Figure S1. Correlation, selectivity, decoder performance, and place cell properties in different hippocampal subregions, neuronal subpopulations, and virtual corridor zones (related to Figures 1 & 2)

(A) Supplement to Fig. 1H (left). Pairs of spatial activity maps of all spatially modulated dentate gyrus neurons sorted by the position of maximal activity in the left map of each pair (normalized per cell). Left pair, sessions in F were split into even and odd lap crossings. Middle pair, sessions in N were split into even and odd lap crossings. Right pair, comparison of lap crossings in F and N (54 sessions from 7 mice).

(B) Population vector (PoV) correlation across mean spatial activity maps for all spatially modulated cells against the position of the animals in the virtual corridor.

(C) Supplement to Fig. 1H (right). Same as (A) but for CA1 (29 sessions from 7 mice).

(D) Same analysis as in (B), but for CA1.

(E) Supplement to Fig. 1J. Spatial decorrelation, quantified as the difference between spatial correlations using Pearson's R within the same familiar (F even–odd) and different environments (FN), in the DG and in CA1 (DG, 0.47 ± 0.03; n = 7; CA1, 0.25 ± 0.05; n = 6; linear mixed model, P = 0.002). Symbols with error bars represent mean ± sem of individual animals, grey circles represent recording sessions.

(F) Comparison of the place field sizes between dentate gyrus and CA1. Left: Place field size of place cells active in the familiar environment (F; DG, 29.66 ± 1.08 cm, n = 7 mice; CA1, 32.59 ± 1.39 cm, n = 7 mice; linear mixed model, P = 0.04). Right: Place field size of place cells active in the novel environment (N; DG, 33.24 ± 1.94 cm, n = 7 mice; CA1, 30.96 ± 1.51 cm, n = 7 mice; linear mixed model, P = 0.89). Same symbols as in panel E.

(G) Complement to Figure 2B. Absolute selectivity for the two environments F and N in DG and CA1 excluding spatially modulated cells (DG, 0.75 ± 0.02; n = 7 mice; CA1, 0.59 ± 0.05; n = 6 mice; linear mixed model, P = 0.002). Same symbols as panel E.

(H) Complement to Figure 2B. Absolute selectivity for the two environments F and N in DG and CA1 only including spatially modulated cells (DG, 0.65 ± 0.08; n = 7 mice; CA1, 0.56 ± 0.05; n = 6 mice; linear mixed model, P = 0.31). Same symbols as in panel E.

(I) Complement to Figure 2C. Absolute selectivity for DG and CA1 neurons plotted against their firing rate, excluding highly selective cells (absolute selectivity >0.99).

(J) Quantification of the decoder performance (AUC) in the dentate gyrus and CA1 excluding spatially modulated cells (DG, 0.55 ± 0.02, n = 7 mice; CA1, 0.49 ± 0.01, n = 6 mice; linear mixed model, P = 0.007). Same symbols as in panel E.

(K) Quantification of the decoder performance (AUC) in the dentate gyrus and CA1 including only the spatially modulated cells (DG, 0.74 ± 0.05, n = 6 mice; CA1, 0.67 ± 0.02, n = 6 mice; linear mixed model, P = 0.17). Same symbols as in panel E.

(L) Quantification of the decoder performance (AUC) in the dentate gyrus and CA1 excluding the reward zone in both environments (DG, 0.66 ± 0.04, n = 6 mice; CA1, 0.56 ± 0.03, n = 6 mice; linear mixed model, P = 0.03). Same symbols as in panel E.

ns, not statistically significant; *, P < 0.05; **, P < 0.01.

Figure S2

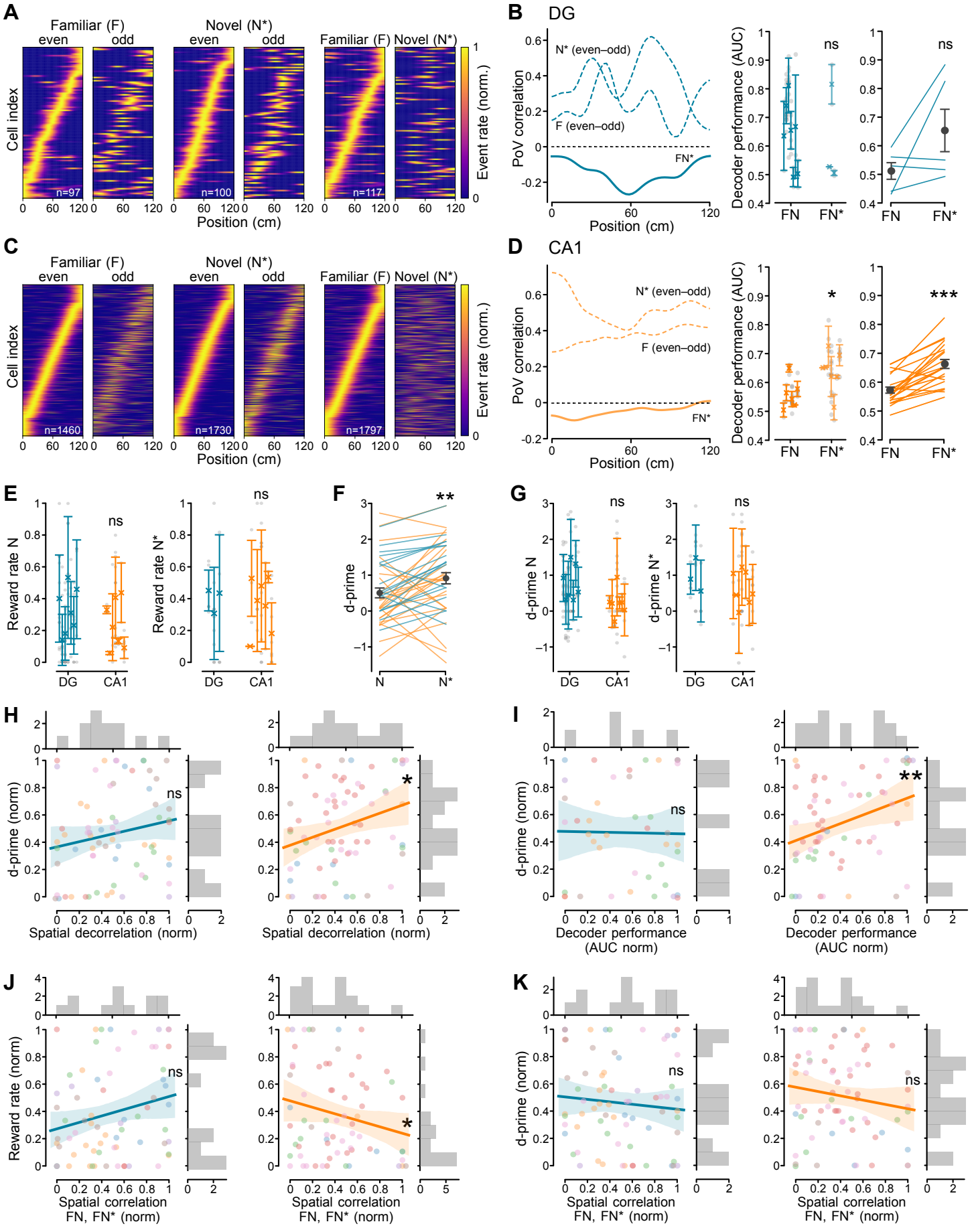
A
Familiar (F)
Novel (N*)
even
odd
Cell index
n=97
n=100
n=117
Event rate (norm.)
Position (cm)
B
DG
N* (even–odd)
F (even–odd)
FN*
PoV correlation
Decoder performance (AUC)
ns
FN
FN*
C
n=1460
n=1730
n=1797
D
CA1
*
***
E
Reward rate N
Reward rate N*
DG
CA1
F
**
d-prime
N
N*
G
d-prime N
d-prime N*
H
d-prime (norm)
Spatial decorrelation (norm)
I
Decoder performance (AUC norm)
J
Reward rate (norm)
Spatial correlation FN, FN* (norm)
K

Figure S2. Neuronal discrimination of highly distinct environments reflects behavioral discrimination in CA1, but not in the dentate gyrus (related to Figure 3)

(A) Pairs of spatial activity maps of all spatially modulated cells in familiar (F) or novel (N*) environments sorted by the position of maximal activity in the left map of each pair (normalized for each cell) for familiar laps (left), novel laps (middle) or familiar vs novel laps (right), recorded from the dentate gyrus (20 sessions from 3 mice).

(B) Left: Population vector correlation (PoV) across mean spatial activity maps for all spatially modulated cells against the position of the animals in the virtual corridor. Middle: Quantification of the decoder performance in the dentate gyrus comparing the prediction between environments FN and FN* (FN, 0.65 ± 0.04, n = 7 mice; FN*, 0.56 ± 0.03, n = 3 mice; linear mixed model, P = 0.75). Symbols with error bars represent mean ± s.e.m. of individual animals, grey circles represent recording sessions. Right: Paired quantification of the decoder performance (AUC) in the dentate gyrus comparing the prediction between environments FN and FN* (FN, 0.52 ± 0.02; FN*, 0.61 ± 0.07; n = 5 sessions; Wilcoxon test, t = 2, P = 0.14). Lines represent paired sessions.

(C) Same as in (A), but for CA1 (20 sessions from 7 mice).

(D) Same analysis as in (B), but for CA1. Left: Population vector correlation (PoV) across mean spatial activity maps. Middle: Decoder performance (FN, 0.56 ± 0.02, n = 6 mice; FN*, 0.63 ± 0.03, n = 7 mice; linear mixed model, P = 0.02). Right: Paired decoder performance (FN, 0.57 ± 0.01; FN*, 0.66 ± 0.02; n = 20 sessions; Wilcoxon test, t = 4, P = 0.0002).

(E) Supplement to Figure 3C. Comparison of behavioral performance (reward rate) in animals implanted for dentate gyrus or CA1 imaging in novel N (left: DG, 0.32 ± 0.06, n = 7 mice; CA1, 0.24 ± 0.06, n = 7 mice; linear mixed model, P = 0.43) and novel N* environments (right: DG, 0.40 ± 0.05, n = 3 mice; CA1, 0.37 ± 0.07, n = 7 mice; linear mixed model, P = 0.95). Symbols with error bars represent mean ± s.e.m. of individual animals, grey circles represent recording sessions.

(F) Quantification of the behavioral performance in the novel (N and N*) environments, measured as d-prime (see Methods). Blue lines refer to single sessions of DG implanted animals, orange lines refer to single sessions of CA1 implanted animals, and dark grey circles represent mean ± s.e.m. (N, 0.50 ± 0.13; in N*, 0.91 ± 0.15, n = 42 sessions, Wilcoxon test, t = 235, P = 0.007).

(G) Comparison of behavioral performance (d-prime) in animals implanted for dentate gyrus or CA1 imaging in novel N (left: DG, 0.76 ± 0.02, n = 7 mice; CA1, 0.23 ± 0.14, n = 7 mice; linear mixed model, P = 0.08) and novel N* environments (right: DG, 0.98 ± 0.27, n = 3 mice; CA1, 0.64 ± 0.18, n = 7 mice; linear mixed model, P = 0.36). Same symbols as in panel E.

(H) Correlation between behavioral performance (d-prime) and spatial decorrelation in the dentate gyrus (left: n = 7 mice and 70 sessions; Pearson's r = 0.19; linear mixed model, P = 0.11) and CA1 (right: n = 7 mice and 69 sessions; Pearson's r = 0.28; linear mixed model, P = 0.01).

(I) Correlation between behavioral performance, (d-prime) within the novel environments (N and N*) and decoder performance in the dentate gyrus (left: n = 7 mice and 41 sessions; Pearson's r = –0.02; linear mixed model, P = 0.92) and CA1 (right: n = 7 mice and 61 sessions; Pearson's r = 0.34; linear mixed model, P = 0.004).

(J) Correlation between behavioral performance (reward rate) and spatial correlation between familiar (F) and novel (N or N*) environments in the dentate gyrus (left: n = 7 mice and 41 sessions; Pearson's r = 0.23; linear mixed model, P = 0.15) and in CA1 (right: n = 7 mice and 61 sessions; Pearson's r = –0.22; linear mixed model, P = 0.04).

(K) Correlation between behavioral performance (d-prime) and spatial correlation between familiar (F) and novel (N or N*) environments in DG (left: n=7 mice and 70 sessions; Pearson's r = –0.09; linear mixed model, P = 0.42) and in CA1 (right: n = 7 mice and sessions; Pearson's r = –0.15; linear mixed model, P = 0.16).

ns, not statistically significant; *, P < 0.05; **, P < 0.01; ***, P < 0.001.

Figure S3

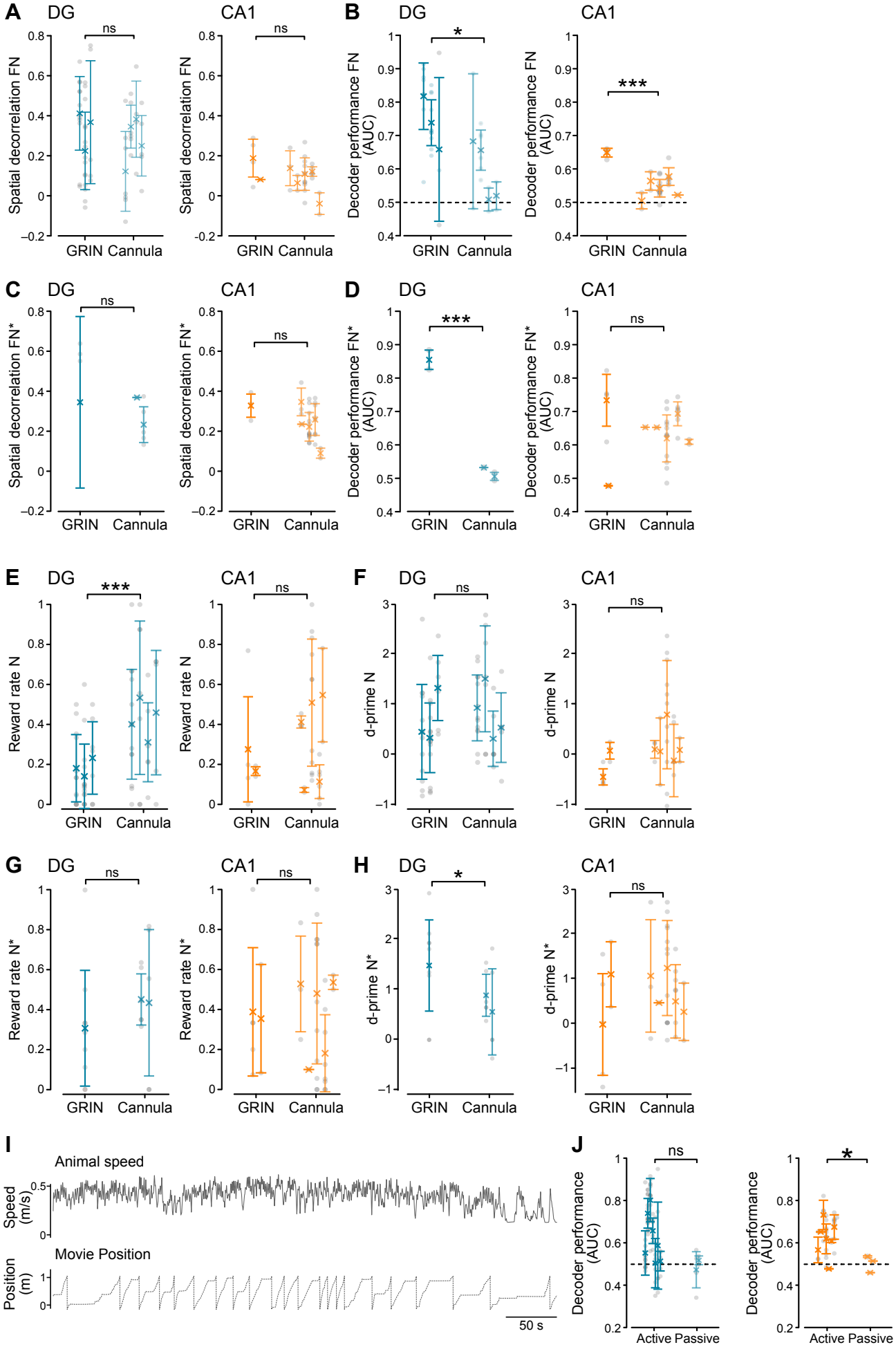
A
DG
CA1
B
DG
CA1
Spatial decorrelation FN
Decoder performance FN (AUC)
ns
*
***
GRIN
Cannula
C
DG
CA1
D
DG
CA1
Spatial decorrelation FN*
Decoder performance FN* (AUC)
E
DG
CA1
F
DG
CA1
Reward rate N
d-prime N
G
DG
CA1
H
DG
CA1
Reward rate N*
d-prime N*
I
Animal speed
Speed (m/s)
Movie Position
Position (m)
50 s
J
Decoder performance (AUC)
Active
Passive

Figure S3. Comparison of imaging and behavioral data using different imaging techniques and behavioral paradigms (related to Figures 1 and 3)

(A-H) Comparison of imaging and behavioral data obtained from animals implanted with GRIN lenses or cannula windows. Data presented in the main figures 1–3 were split according to implant type.

(A) Spatial decorrelation in the dentate gyrus (left, GRIN FN: 0.33 ± 0.05, *n* = 3 mice and 32 sessions; cannula, FN, 0.27 ± 0.06, *n* = 4 mice and 22 sessions; linear mixed model, *P* = 0.99) and CA1 (right, GRIN FN: 0.13 ± 0.05, *n* = 2 mice and 5 sessions; cannula, FN, 0.08 ± 0.03, *n* = 5 mice and 24 sessions; linear mixed model, *P* = 0.17). Symbols with error bars represent mean ± sem of individual animals, grey circles represent recording sessions.

(B) Decoder performance (AUC) in the dentate gyrus (left, GRIN FN: 0.74 ± 0.04, *n* = 3 mice; cannula FN: 0.59 ± 0.04, *n* = 4 mice; linear mixed model, *P* = 0.01) and CA1 (right, GRIN FN: 0.65 ± 0.01, *n* = 1 mouse; cannula FN: 0.54 ± 0.01, *n* = 5 mice; linear mixed model, *P* = 0.0003). Same symbols as in panel A.

(C) Spatial decorrelation in the dentate gyrus (left, GRIN FN*: 0.34 ± 0.24, *n* = 1 mouse; cannula, FN*, 0.30 ± 0.07, *n* = 2 mice; linear mixed model, *P* = 0.69) and CA1 (right, GRIN FN*: 0.33 ± 0.04, *n* = 1 mouse; cannula, FN*, 0.23 ± 0.04, *n* = 5 mice; linear mixed model, *P* = 0.33). Same symbols as in panel A.

(D) Decoder performance (AUC) in the dentate gyrus (left, GRIN FN*: 0.85 ± 0.03, *n* = 1 mouse; cannula, FN*, 0.52 ± 0.01, *n* = 2 mice; linear mixed model, $P = 4*10^{-46}$) and CA1 (right, GRIN FN*: 0.61 ± 0.13, *n* = 2 mice; cannula, FN*, 0.64 ± 0.01, *n* = 5 mice; linear mixed model, *P* = 0.68). Same symbols as in panel A.

(E) Behavioral performance measured as reward rate in the novel N environment in the dentate gyrus (GRIN, 0.18 ± 0.03, *n* = 3; cannula, 0.42 ± 0.05, *n* = 4; linear mixed model, $P = 3*10^{-6}$) and CA1 (GRIN, 0.18 ± 0.04, *n* = 2; cannula, 0.26 ± 0.08, *n* = 5; linear mixed model, *P* = 0.51). Same symbols as in panel A.

(F) Behavioral performance measured as d-prime in the novel N environment in the dentate gyrus (GRIN, 0.69 ± 0.31, *n* = 3; cannula, 0.80 ± 0.26, *n* = 4; linear mixed model, *P* = 0.65) and CA1 (GRIN, -0.04 ± 0.26, *n* = 2; cannula, 0.33 ± 0.16, *n* = 5; linear mixed model, *P* = 0.24). Same symbols as in panel A.

(G) Behavioral performance measured as reward rate in the novel N* environment in the dentate gyrus (GRIN, 0.31 ± 0.10, *n* = 1; cannula, 0.44 ± 0.01, *n* = 2; linear mixed model, *P* = 0.30) and CA1 (GRIN, 0.37 ± 0.02, *n* = 2; cannula, 0.36 ± 0.09, *n* = 5; linear mixed model, *P* = 0.98). Same symbols as in panel A.

(H) Behavioral performance measured as d-prime in the novel N* environment in the dentate gyrus (GRIN, 1.41 ± 0.32, *n* = 1; cannula, 0.72 ± 0.16, *n* = 2; linear mixed model, *P* = 0.04) and CA1 (GRIN, 0.52 ± 0.56, *n* = 2; cannula, 0.68 ± 0.19, *n* = 5; linear mixed model, *P* = 0.33). Same symbols as in panel A.

(I-J) Hippocampal neuronal discrimination requires active spatial navigation

(I) Representative open-loop recording session showing the speed of the animal on the running wheel (top trace), and the uncoupled position on the virtual reality track, as imposed by a pre-recorded virtual-reality session (bottom dotted trace).

(J) Quantification of the decoder performance (AUC) comparing active and passive spatial navigation conditions in DG (left: active condition, 0.65 ± 0.04, *n* = 7 mice; passive condition, 0.47 ± 0.01, *n* = 3 mice; linear mixed model, *P* = 0.17), and CA1 (right: active condition, 0.63 ± 0.03, *n* = 6 mice; passive condition, 0.52 ± 0.01, *n* = 3 mice; linear mixed model, *P* = 0.01). Symbols with error bars represent mean ± sem of individual animals, grey circles represent recording sessions. Note that for the DG, the reduction in decoder performance does not reach statistical significance.

ns, not statistically significant; *, $P < 0.05$; ***, $P < 0.001$.

Figure S4

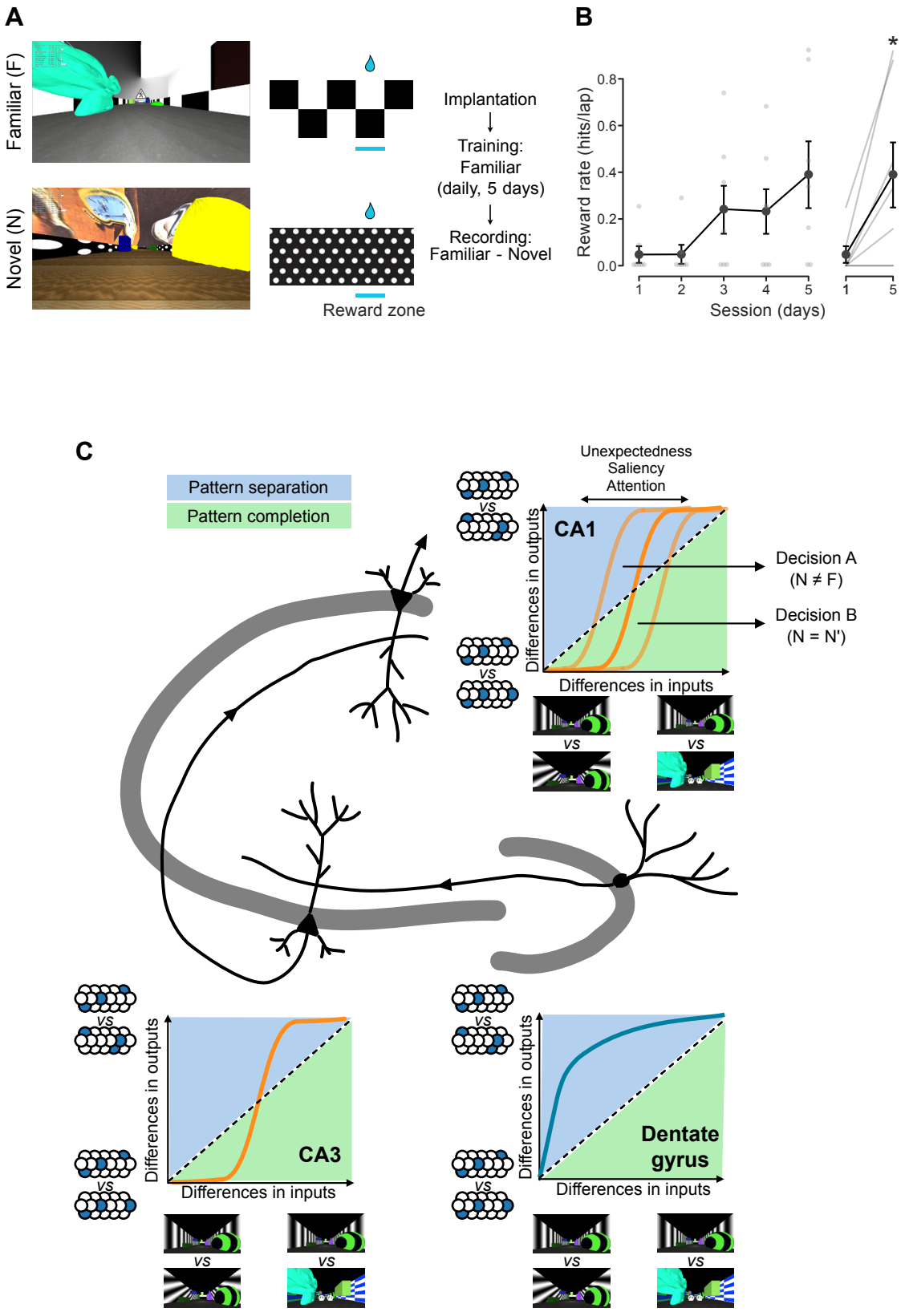
A
Familiar (F)
Novel (N)
Reward zone
Implantation
Training:
Familiar
(daily, 5 days)
Recording:
Familiar - Novel
B
Reward rate (hits/lap)
Session (days)
*
C
Pattern separation
Pattern completion
Unexpectedness
Saliency
Attention
CA1
CA3
Dentate
gyrus
Differences in outputs
Differences in inputs
Decision A
(N ≠ F)
Decision B
(N = N')
VS

Figure S4. Behavioral training and virtual-reality environments used during whole-cell recordings, and schematic synthesis of neuronal and behavioral discrimination in the hippocampal circuit (related to Figure 4)

(A) Left: views of the familiar (F) and novel (N) virtual reality environments. Middle: schematic indicating the reward locations along the corridor. Right: experimental timeline.
(B) Left: progression of the behavioral performance during learning of the task in the familiar (F) virtual environment, measured as reward rate (hits per lap). Small grey circles represent individual animals, while large circles indicate mean ± s.e.m. across all animals. Right: comparison of behavioral performance during the first and the last training sessions in the familiar environment (0.05 ± 0.03 and 0.39 ± 0.13, respectively; $n = 7$, Wilcoxon test, $t = 0$, $P = 0.043$).
(C) Schematic synthesis of neuronal and behavioral discrimination in the hippocampal circuit. The dentate gyrus generates robustly decorrelated neuronal representations of different environments, even if the differences are small. Attractor dynamics in area CA3 lead to a sharp transition from pattern separation to completion, instructed by the decorrelated information from the dentate gyrus, as the differences in its inputs exceed a threshold. CA1 integrates inputs from CA3 with several additional inputs mediating the unexpectedness and saliency of the environment. The final representation in CA1 is then used by downstream neocortical circuits to guide learning and behavioral decisions.

Table S1. Linear mixed model results (related to Figures 1–3)

Quantity	Figure	Coef.	Std.Err.	z	P	[0.025	0.975]
Spatial decorrelation	1J	-0.192	0.063	-3.026	0.002	-0.316	-0.068
Absolute selectivity	2B	-0.149	0.044	-3.388	0.0007	-0.236	-0.063
Decoder perfomance (AUC)	2D	-0.104	0.051	-2.044	0.041	-0.204	-0.004
Spatial decorrelation	3E	-0.001	0.098	-0.008	0.994	-0.193	0.192
Spatial decorrelation	3G	0.148	0.042	3.559	0.0004	0.066	0.229
Reward rate - Spatial decorrelation (DG)	3H	-0.041	0.129	-0.319	0.750	-0.295	0.212
Reward rate - Spatial decorrelation (CA1)	3H	0.491	0.117	4.185	0.0002	0.261	0.721
Reward rate - Decoder performance (DG)	3I	-0.010	0.171	-0.057	0.955	-0.345	0.326
Reward rate - Decoder performance (CA1)	3I	0.257	0.125	2.053	0.040	0.012	0.501